

Resonating valence bond wave function for the two dimensional fractional spin liquid

S. Yunoki and S. Sorella

INFN-Democritos, National Simulation Centre, and SISSA, I-34014 Trieste, Italy

(Dated: February 7, 2020)

The unconventional low-lying spin excitations, recently observed in neutron scattering experiments on Cs_2CuCl_4 , are explained with a spin liquid wave function. The dispersion relation as well as the wave vector of the incommensurate spin correlations are well reproduced within a projected BCS wave function with gapless and fractionalized spin-1/2 excitations around the nodes of the BCS gap function. The proposed wave function is shown to be very accurate for one-dimensional spin-1/2 systems, and remains similarly accurate in the two-dimensional model corresponding to Cs_2CuCl_4 , thus representing a good ansatz for describing spin fractionalization in two dimensions.

PACS numbers: 74.20.Mn, 71.10.Hf, 75.10.Jm, 71.27.+a

The fractionalization of spin excitations in one-dimensional (1D) spin-1/2 antiferromagnetic (AF) Heisenberg systems was conjectured by Faddeev and Takhtajan [1] more than 20 years ago, and by now the concept of "spinons", as spin-1/2 elementary excitations for 1D quantum AF systems, has been well established both theoretically [2] and experimentally [3].

An important and intriguing issue raised by Anderson [4] after the discovery of high- T_C superconductors (HTSC) is whether fractionalized gapless spinons can be defined even in higher dimensions. Many theoretical studies have been done so far analytically [5] and numerically [6], mainly by considering weakly coupled chains. Most studies suggest that unconventional 1D features are very unlikely to occur in higher dimensions since more conventional states, *e.g.*, magnetically ordered, are stabilized with a weak inter-chain coupling.

The same question can be also addressed experimentally. A series of recent inelastic neutron scattering (INS) experiments on Cs_2CuCl_4 by Coldea *et al* [7, 8] showed that, as in 1D systems [3], the INS spectrum on this material consists of a broad incoherent continuum at each momentum, a fingerprint of spin fractionalization, despite the fact that the system is clearly two-dimensional (2D). It was also found that the system is described by the following 2D spin-1/2 AF Heisenberg model (2DAFHM) on the triangular lattice (see Fig. 1a):

$$H = J \sum_{\langle i,j \rangle} \vec{S}_i \cdot \vec{S}_j + J' \sum_{\langle\langle i,j \rangle\rangle} \vec{S}_i \cdot \vec{S}_j \quad (1)$$

with the intra-chain coupling $J = 0.374$ meV and the inter-chain coupling $J'/J = 0.33$ [7]. Here the symbol $\langle i,j \rangle$ ($\langle\langle i,j \rangle\rangle$) indicates nearest neighbor (n.n.) sites along the chain (between different chains). Additional terms such as the Dzyaloshinskii-Moriya interaction and the coupling in the third direction, both of the same order $\simeq 0.02$ meV [8], are certainly relevant to explain the various low-temperature phases [7]. However in this study we ignore these much smaller terms as our main purpose is to determine the minimal model and its ground state (GS) wave function (WF) which may lead to spin frac-

tionalization in the 2D system.

In this Letter we propose a projected BCS WF for the GS of Eq. (1): $|\Phi\rangle = \hat{\mathcal{P}}|\text{BCS}\rangle$, where $|\text{BCS}\rangle$ is the GS of the following mean-field BCS Hamiltonian,

$$H_{\text{BCS}} = \sum_{\mathbf{k},s} \xi_{\mathbf{k}} c_{\mathbf{k},s}^\dagger c_{\mathbf{k},s} + \sum_{\mathbf{k}} \left[\Delta_{\mathbf{k}} c_{\mathbf{k},\uparrow}^\dagger c_{-\mathbf{k},\downarrow}^\dagger + \text{h.c.} \right]. \quad (2)$$

Here $\xi_{\mathbf{k}} = \epsilon_{\mathbf{k}} - \mu$, $\epsilon_{\mathbf{k}} = -2 \cos(\mathbf{k} \cdot \vec{\tau}_1)$, μ is the chemical potential, $c_{\mathbf{k},s}^\dagger$ the creation operator of an electron with momentum \mathbf{k} and spin $s = \pm 1/2$, and $\Delta_{\mathbf{k}}$ the real gap function for singlet pairing. The variational state $|\Phi\rangle$ for the spin Hamiltonian H is obtained by applying to $|\text{BCS}\rangle$ the Gutzwiller projector $\hat{\mathcal{P}}$ onto the subspace of singly occupied sites. The quantities $\Delta_{\mathbf{k}}$ and μ are determined following the variational principle, *i.e.*, by minimizing the energy $E(\Phi) = \langle \Phi | H | \Phi \rangle / \langle \Phi | \Phi \rangle$. Since the short range terms are more relevant for this purpose, the Fourier transform of $\Delta_{\mathbf{k}}$ is truncated up to the third distance along the chain so that 10 independent parameters for $\Delta_{\mathbf{k}}$ are optimized along with μ [9, 10]. Note that whenever μ is finite, H_{BCS} no longer possesses particle-hole symmetry and therefore $|\Phi\rangle$ violates the Marshall sign rule [11]. In the following, coupled L -site chains for a total number $N = L^2$ of sites with periodic boundary conditions are used unless otherwise stated. Moreover, in order to judge the quality of $|\Phi\rangle$, the variance of the energy, $\sigma^2(|\Phi\rangle) = \langle \Phi | (H - E(\Phi))^2 | \Phi \rangle / \langle \Phi | \Phi \rangle$ [12], is also calculated. For comparison the same spin liquid WF $|\Phi\rangle$ is applied to other models, the uncoupled Heisenberg chains with $J' = 0$ and the 2DAFHM on the square lattice (See Fig. 1a). For each model the gap function $\Delta_{\mathbf{k}}$ and μ are optimized independently.

The main point of this Letter is that the variational approach represents an accurate theoretical tool for extending the notion of spinons in higher dimensions. With this approach we are able to reproduce the qualitative as well as the quantitative features of the experiments, confirming the possibility of spin fractionalization in 2D, with a transparent theoretical framework. Following Wen [13], we also show that the excitations of H_{BCS} are related to the physical excitations of the spin Hamiltonian.

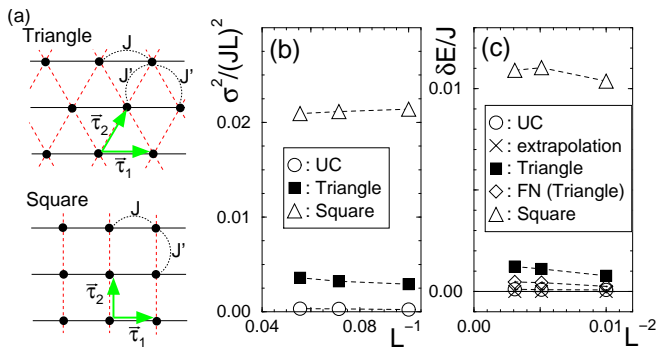


FIG. 1: (a) Lattice geometries studied. The n.n. exchange coupling is fixed at $J'/J = 0.33$. $\bar{\tau}_1$ and $\bar{\tau}_2$ are the primitive translational vectors. (b) Variance of energy $\sigma^2(|\Phi\rangle)$ for $N = L \times L$ clusters. (c) Estimate of the variational error in the energy per site. The FN variational error for the triangular lattice and the variance extrapolated error for UC are also plotted.

Let us first start with the 1D spin-1/2 AF Heisenberg model (1DAFHM) with n.n. coupling, to show that the spin liquid characteristics in 1D are well described by the WF $|\Phi\rangle$. It is already known [14, 15] that $|\Phi\rangle$ describes almost exactly the GS, *e.g.*, with an accuracy in the energy of about one part over 10^4 and spin correlation functions with the right power law decay ($\sim r^{-1}$) as a function of distance r [16]. For the 1D model, the optimized μ is zero and therefore the BCS spectrum $E_{\mathbf{k}} = \sqrt{\xi_{\mathbf{k}}^2 + \Delta_{\mathbf{k}}^2}$ of Eq. (2) has gapless excitations at $\mathbf{k} = \pm\pi/2$, exactly as the spinon spectrum of 1DAFHM does [2]. Thus, it appears possible to construct the low-lying excited states from $|\Phi\rangle$ and to reproduce the well known spinon spectrum for 1DAFHM. Indeed, the elementary excitations of H_{BCS} with energy $E_{\mathbf{k}}$ are described by the standard Bogoliubov modes, $\gamma_{\mathbf{k},s}^\dagger$. Therefore the simplest variational state for the spinon at momentum \mathbf{k} is $|\mathbf{k}\rangle = \hat{\mathcal{P}}\gamma_{\mathbf{k},\downarrow}^\dagger|\text{BCS}\rangle$. To see whether this state $|\mathbf{k}\rangle$ corresponds to a spinon state, we consider a ring with *odd* number of sites $L = 31$ and z -component of the total spin $S_z^{\text{tot}} = -1/2$. For this case it is known that a well defined spinon exists only for half of the total Brillouin zone ($\pi/2 \leq |\mathbf{k}| \leq \pi$). As shown in Fig. 2, in this branch, the WF $|\mathbf{k}\rangle$ represents fairly well the excited state with a spinon at momentum \mathbf{k} , as can be verified by the good accuracy in energy and the small variance $\sigma^2(|\mathbf{k}\rangle)$. Notice that, although the projection $\hat{\mathcal{P}}$ is crucial to gain a quantitative agreement for the spectrum, the BCS spectrum $E_{\mathbf{k}}$ already gives a qualitatively correct feature of gapless excitations with finite spin-wave velocity at the right momentum $\mathbf{k} = \pi/2$ (see Fig. 2). For the remaining branch of momenta ($|\mathbf{k}| \leq \pi/2$), the excitations for 1DAFHM are no longer elementary [2]. As shown in Fig. 2, though the state $|\mathbf{k}\rangle$ is formally defined even for these momenta, it represents a poor rep-

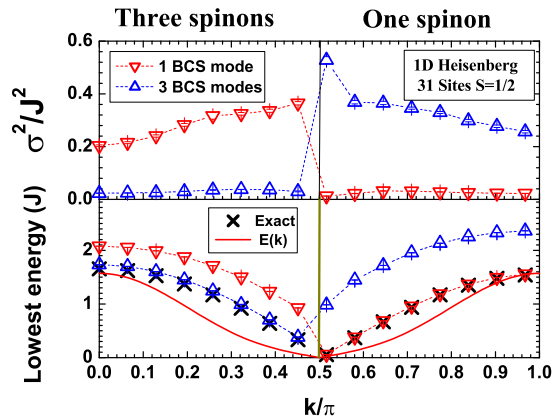


FIG. 2: Lower panel: lowest energy spin-1/2 excitations of the 1DAFHM as a function of momentum \mathbf{k} . Upper panel: the variance σ^2 of the projected BCS excitations (see text). Solid line is the BCS spectrum $E_{\mathbf{k}}$ scaled by a factor to match the exact bandwidth, other lines are guides to the eye.

resentation for the exact excited state. In fact $E(\mathbf{k})$ becomes quite off from the exact value, and $\sigma^2(|\mathbf{k}\rangle)$ considerably increases as soon as the momentum crosses the "spinon Fermi surface" at $\mathbf{k} = \pi/2$. Remarkably, by projecting a non-elementary excitation of H_{BCS} , namely $\hat{\mathcal{P}}\gamma_{\mathbf{k}_F,\downarrow}^\dagger\gamma_{-\mathbf{k}_F,\downarrow}^\dagger\gamma_{\mathbf{k},\uparrow}^\dagger|\text{BCS}\rangle$ with $\mathbf{k}_F = \pi(L+1)/2L$, which mimics the correct 3-spinons eigenstate, we can achieve a good agreement of the spectrum even in the region outside the spinon Fermi surface (see Fig. 2, up-triangles). Within the present variational scheme, a way to define the spinon Fermi surface is obtained simply by switching off the pairing function $\Delta_{\mathbf{k}}$ adiabatically. The elementary excitation which survives after the projection is generated by destroying (creating) a particle only inside (outside) the Fermi surface, determined by $\xi_{\mathbf{k}} = 0$.

Let us now extend our variational analysis to the 2DAFHM. The most important effect of frustration on the proposed WF $|\Phi\rangle$ is to change μ to a nonzero value. This should be contrasted to the case of 2DAFHM on the square lattice with no frustration such as the one shown in Fig. 1a, where the optimized μ is always zero. Therefore the Marshall sign rule for the state $|\Phi\rangle$ is violated on the triangular lattice, and the gapless excitations of H_{BCS} are no longer located at commensurate points. For example, the optimized value for $N = 18 \times 18$ is $\mu = 0.110(4)$. Thus one can make a spin-1 gapless excitation at wave vector $Q_x = 2\cos^{-1}(-\mu/2) \sim 1.035(2)\pi$, which is close to the experimentally observed incommensurate wave vector on Cs_2CuCl_4 [7]. Indeed the nodal lines of $\Delta_{\mathbf{k}}$ intersect the lines defined by $\xi_{\mathbf{k}} = 0$, leading to four gapless modes related by mirror symmetries for the BCS spectrum $E_{\mathbf{k}}$.

To check the quality of the proposed wave function

$|\Phi\rangle$, the variance $\sigma^2(|\Phi\rangle)$ is calculated in Fig. 1b, where for comparison the variances are also presented for uncoupled chains (UC) with $J' = 0$ (spin liquid) and for 2DAFHM on the square lattice with $J'/J = 0.33$ (non spin liquid). As seen in Fig. 1b, the variance for the triangular case is much smaller than the variance corresponding to the square lattice and instead this value is similar to the one for UC. In order to confirm the quality of the WF further, we calculate the error of the estimated energy from the exact value e_0 : $\delta E = E(\Phi)/N - e_0$. Since the exact energy for the triangular lattice case is not known, we estimate e_0 by extrapolating to zero variance the variational energies corresponding to $|\Phi\rangle$ and to the one Lanczos step WF $|\Phi_{1LS}\rangle = (1 + \alpha H)|\Phi\rangle$ with optimized α [9]. Indeed this procedure works well for UC as shown in Fig. 1c. Though the WF $|\Phi\rangle$ for the triangular lattice is not as accurate as for UC it remains of high quality, much better than the corresponding square lattice case. This is remarkable as even for the square lattice the estimate of the energy is fairly good (only $\sim 0.01J$ per site off).

Though the variational approach can provide accurate upper bounds for the energy, it may suffer the well known difficulty that the low energy modes are usually insensitive to the total energy, and sometimes completely different WF's give more or less the same energy [17]. In order to reduce this difficulty, quantum Monte Carlo methods, such as a recently developed fixed node (FN) technique, may be used [9, 18]. Within this more powerful FN approach, the variational scheme is used to determine only the signs of the wave function $\psi_G(x) = \langle x|\Phi\rangle$ on each configuration x of electrons. In this basis $|x\rangle$ all the matrix elements of the Hamiltonian such that $s_{x',x} = \psi_G(x')\langle x'|H|x\rangle\psi_G(x) < 0$ are considered exactly. Instead all the off-diagonal matrix elements with $s_{x',x} > 0$ are treated semiclassically and traced to the diagonal term, leading to an effective FN Hamiltonian H_{FN} . Since the semiclassical approximation is usually good at low energy, we believe that this approach provides a sensible test to examine the stability of the variational WF at low energy. Moreover the FN energy is variational [9, 18], and, as shown in Fig. 1c, is much better than the variational estimate $E(\Phi)$.

In Fig. 3, the real space spin correlation functions are calculated for 2DAFHM on both the triangular and square lattices. For the square geometry, it is clear that the FN approach considerably enhances the large distance correlations, suggesting that the spin liquid state is unstable toward AF long-range order, in agreement with previous studies [6]. A completely different scenario is evident for the triangular geometry where these long distance correlations do not appreciably change with respect to the variational $|\Phi\rangle$, strongly indicating that the spin liquid state $|\Phi\rangle$ is stable, namely close to the exact GS, at least for the clusters studied. It appears that, whenever the H_{BCS} contains gapless modes at incommensurate \mathbf{k} ,

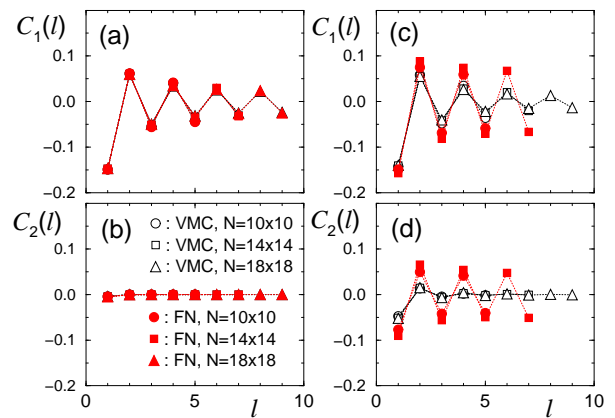


FIG. 3: Real space spin correlation function (z -component) $C_i(l) = \langle S_z(\vec{r})S_z(\vec{r} + l\vec{\tau}_i) \rangle$ as a function of distance for the 2DAFHM with $J'/J = 0.33$ on the triangular lattice (a,b) and on the square lattice (c,d) for the variational (open marks) and FN (solid marks) approximations. Lines are guides to the eye.

these modes may remain stable against fluctuations, and define a nonconventional liquid state with gapless spin excitations not protected by the broken symmetry.

Encouraged by the above results, we now consider the low-lying excitations on the spin liquid state $|\Phi\rangle$ for the 2DAFHM on the triangular lattice. Analogously to the 1DAFHM, the spin-1 excitation spectrum can be estimated using $E_{\mathbf{k}}$, with the optimized variational parameters. The lower energy threshold is obtained by minimizing the energy of two BCS modes: $E_{S=1}(\mathbf{k}) = E_{\mathbf{q}} + E_{\mathbf{k}-\mathbf{q}}$, with varying \mathbf{q} under the spinon Fermi surface condition (FSC): $\xi_{\mathbf{q}} < 0$ and $\xi_{\mathbf{k}-\mathbf{q}} \geq 0$. Analogously, the high energy threshold is estimated by maximizing the above energy $E_{S=1}(\mathbf{k})$. The results are plotted in Fig. 4a by solid lines. As in the 1DAFHM, we can capture the qualitatively correct features if we assume the FSC for $E_{S=1}(\mathbf{k})$, since only with this condition both the low and high energy thresholds of the INS data on Cs_2CuCl_4 [7] can be qualitatively reproduced (see Fig. 4a).

In order to estimate quantitatively the low energy excitations of our spin liquid state $|\Phi\rangle$, we finally compute the spin-1 excitation spectrum in the correct projected Hilbert space by using the FN method. Due to the quality of our WF $|\Phi\rangle$ and to the fact that the FN approximation is exact for 1DAFHM, we expect that this approach should give a reliable description of the exact excitation spectrum of H . By using the forward walking technique [19], one can evaluate the imaginary time (τ) evolution of the following quantity:

$$S(\mathbf{k}, \tau) = \frac{\langle \Phi | S_z(\mathbf{k}) e^{-\tau H_{FN}} S_z(-\mathbf{k}) | \psi_0 \rangle}{\langle \Phi | e^{-\tau H_{FN}} | \psi_0 \rangle}, \quad (3)$$

where $S_z(\mathbf{k}) = \sum_{\mathbf{r}} e^{i\mathbf{k}\cdot\mathbf{r}} S_z(\mathbf{r}) / \sqrt{N}$ and $|\psi_0\rangle$ is the ground

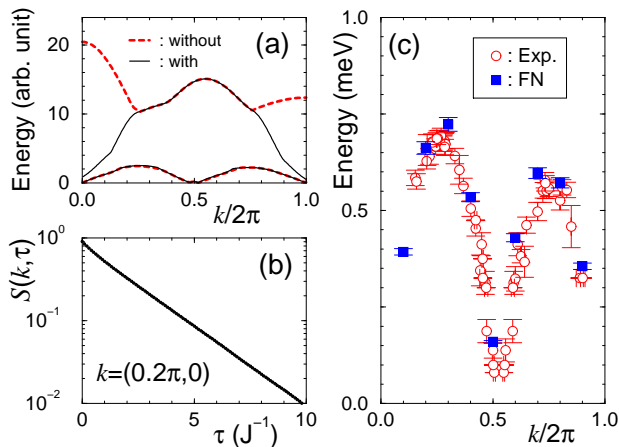


FIG. 4: (a) Lower and upper thresholds for the spin-1 excitations of H_{BCS} calculated for $\mathbf{k}/\bar{\tau}_1$ with (without) the FSC [solid (dashed) lines] (see the text). (b) A typical semi-log plot of the imaginary time correlation function. (c) The lowest spin-1 excitation energies within the FN approximation for 2DAFHM on the triangular lattice [Eq. (1)] with $N = 10 \times 20$ (solid squares) compared with experimental data on Cs_2CuCl_4 [8] (open circles) along $\mathbf{k}/\bar{\tau}_1$.

state of H_{FN} . By simple inspection, the lowest spin-1 excitation energy $E_{\mathbf{k}}^{S=1}$ of H_{FN} can be obtained by fitting the large τ behavior of $S(\mathbf{k}, \tau) \propto e^{-E_{\mathbf{k}}^{S=1}\tau}$. An example of how the method works is given in Fig. 4b where one can see that $\ln S(\mathbf{k}, \tau)$ is almost linear in τ . Therefore, we can estimate the lowest excitation energy for each \mathbf{k} , and the results are summarized in Fig. 4c, where the experimental data [7] are also displayed. The extremely good agreement suggests that the 2D model of Eq. (1) describes correctly the experiments, thus supporting the appearance of a spin liquid state. Since no sizable magnetic order was found in this 2D model (Fig. 3), it is very likely that the experimentally observed ordered phases at very low temperatures should be due only to 3D effects [8]. We cannot exclude the possibility that a small spin gap could remain in the thermodynamic limit, as our numerical resolution is limited in the available finite size clusters.

In conclusion, we have shown that, comparing several different models, a simple variational approach is capable of describing the GS properties as well as the low-lying excitations of a spin liquid not only for 1D systems but also for a 2D frustrated spin-1/2 system. Within this approach it appears that, when the H_{BCS} spectrum remains gapless at commensurate \mathbf{k} as in an unfrustrated square lattice, the spin fractionalized state undergoes a magnetic instability. On the contrary, when the H_{BCS} spectrum remains gapless at incommensurate \mathbf{k} , as in a frustrated system, it appears much more difficult to destabilize the fractionalized state. It should be emphasized that both

the experimental and the present numerical work consistently suggest that a spin liquid with gapless spin-1/2 excitations appears possible in 2D, its stability being intimately related to the incommensurate momenta of the gapless modes.

Our results may have some impact even for HTSC, where the carrier doping naturally leads to incommensurate nodal Fermi points. The existence of a nodal spin liquid was also conjectured before for interacting Bose systems [20, 21] where a Bose metal is the natural bosonic counterpart of a spin liquid with gapless spin excitations and no magnetic order. Moreover our findings might be also important in view of the recent discovery of superconductivity in $\text{Na}_x\text{CoO}_2 \cdot 1.3\text{H}_2\text{O}$ on the triangular geometry [22]. It is possible that nonconventional superconductivity with anomalous fractionalized phases may be a key ingredient to understand this new material.

We acknowledge R. Coldea for sending us the experimental data and F. Becca for providing us exact diagonalization data. This work is partially supported by INFN-MALODI and MIUR-COFIN 2001.

-
- [1] L. D. Faddeev and L. A. Takhtajan, Phys. Lett. A **85**, 375 (1981).
 - [2] see, e.g., V. E. Korepin, in "Exactly solvable models of strongly correlated electrons", eds. V. E. Korepin and H. L. Essler, World Scientific (1994).
 - [3] D. A. Tennant *et al.*, Phys. Rev. Lett. **70**, 4003 (1993).
 - [4] P. W. Anderson, G. Baskaran, Z. Zou, and T. Hsu, Phys. Rev. Lett. **58**, 2790 (1987).
 - [5] S. P. Strong and A. J. Millis Phys. Rev. Lett. **69**, 2419 (1992); *ibidem*, Phys. Rev. B **50**, 9911 (1994); C. Castellani, C. Di Castro and W. Metzner Phys. Rev. Lett. **72**, 316 (1994); H. J. Schulz Phys. Rev. B **53**, 2959 (1996); P. Kopietz, V. Meden, and K. Schönhammer Phys. Rev. B **56** 7232 (1997).
 - [6] A. W. Sandvik Phys. Rev. Lett. **83**, 3069 (1999).
 - [7] R. Coldea *et al.*, Phys. Rev. Lett. **86**, 1335 (2001); *ibidem*, Phys. Rev. Lett. **88**, 137203 (2002).
 - [8] R. Coldea *et al.*, cond-mat/0307025.
 - [9] S. Sorella Phys. Rev. B **64**, 024512 (2001), *ibidem*, cond-mat/0201388, lecture notes for the Euro-Winter School Kerkade-NL (2002).
 - [10] The nearest-neighbor hoppings along $\bar{\tau}_2$ and $\bar{\tau}_2 - \bar{\tau}_1$ were also optimized and found to be negligibly small.
 - [11] W. Marshall, Proc. R. Soc. London Ser. A **232**, 48 (1955).
 - [12] Only when $|\Phi\rangle$ is an exact eigenstate, $\sigma^2(|\Phi\rangle) = 0$, and the smaller is its value, the better is the quality of $|\Phi\rangle$.
 - [13] X. G. Wen Phys. Rev. B **44**, 2664 (1991).
 - [14] S. Sorella *et al.*, Phys. Rev. Lett. **88**, 117002 (2002).
 - [15] C. Gros Ann. of phys. (N.Y.), **189**, 53 (1989).
 - [16] F. D. M. Haldane Phys. Rev. Lett. **60**, 635 (1988).
 - [17] S. Liang *et al.*, Phys. Rev. Lett. **61**, 365 (1988).
 - [18] D.F.B. ten Haaf *et al.*, Phys. Rev. B **51**, 13039 (1995).
 - [19] M. Calandra and S. Sorella Phys. Rev. B **57**, 11446 (1998).

[20] D. Das and S. Doniach Phys. Rev. B **60**, 1261 (1999).

[21] A. Paramakanti *et al.*, Phys. Rev. B **66** 054526 (2002).

[22] K. Takada *et al.*, Nature **422**, 53 (2003).